



Research paper

Assessment of hydrogeochemical processes in the aquifers of Coimbatore city, India with special reference to nickel contamination

K.L. Priya^{a,*}, Kokkat Aswin^b, M.S. Indu^a, S. Adarsh^a^a Department of Civil Engineering, T.K.M. College of Engineering, Kollam, India^b Water Institute, Karunya Institute of Technology & Sciences, Coimbatore, Tamil Nadu, India

ARTICLE INFO

Keywords:

Groundwater quality
Geochemistry
Rock-water interaction
Textile sewage
Nickel
Coimbatore
India

ABSTRACT

Rapid industrialization of the city of Coimbatore in the recent past has imposed stress on groundwater resources, resulting in quantity depletion and quality deterioration. The present study aimed at evaluating the groundwater quality of Coimbatore city, India. Qualitative analysis of 17 groundwater samples were made during the post-monsoon and pre-monsoon in 2015. As groundwater forms a dominant source for irrigation and domestic purposes, an evaluation of its suitability for these purposes were assessed. Classic geochemical methods have been coupled with geospatial approaches to arrive at the geochemical processes controlling the hydrochemistry of groundwater. The study reveals that the high concentration of Nickel and Total Dissolved Solids in the groundwater is caused due to the contamination from textile mill effluent, which is discharged into the Noyyal river and ultimately join the water table. The influence of this contamination is reflected in the geochemical processes, wherein the contaminated area exhibits different water type at different seasons; Ca-type water was converted to Na-type or mixed Na, Ca-type during the transition from post-monsoon to pre-monsoon. Majority of the samples are influenced by rock-water interaction and the dominance of the processes followed the order ion exchange > weathering > reverse ion exchange. The major driving force for ion exchange between Ca^{2+} in rock and Na^+ in water was the abundance of Na^+ in the percolating water, which is contributed by textile effluent. Among the weathering process, carbonate weathering dominated silicate weathering due to the presence of limestone deposit and red calcareous soil. The quantification of saturation index suggests that carbonate minerals are super saturated in the groundwater in the following order: dolomite > calcite > aragonite, while other minerals including fluorite, halite and gypsum were unsaturated.

1. Introduction

In many arid and semi-arid regions, groundwater is one of the alternate sources mainly for domestic and agricultural activities. Due to rapid industrialization and rising population, stress on the groundwater resource is increasing, on quantitative as well as qualitative aspects. It is the quality of groundwater, which ultimately determines its suitability for various purposes. Groundwater quality may get deteriorated by natural and anthropogenic factors namely geochemical processes (Hem, 1989; Rao et al., 2012), precipitation (Jalali, 2007), leaching of domestic, agricultural and industrial waste. The various geochemical processes which take place between water and aquifer include weathering and dissolution, precipitation and crystallization, sorption, ion exchange and reactions. The interaction of both natural processes and human activities determine the water types (Belkhir and Mouni, 2013).

The knowledge of the geochemical interactions in the soil/rock-groundwater system is essential to an adequate assessment of water quality at a regional scale (Reddy et al., 2010). Further, a thorough understanding of the geochemical process that affect the groundwater quality is necessary to address groundwater-related issues (Subramani et al., 2010).

The assessment of hydrogeochemical processes requires the knowledge of hydrochemical facies, influence of rock-water interactions, evaporation and precipitation on water chemistry, which can be studied using graphical plots such as Piper diagram (Lee et al., 2001; Hajalilou and Khaleghi, 2009; Sadashivaiah et al., 2008; Selvakumar et al., 2017) and Gibbs plot (Kaur et al., 2017; Kozłowski and Komisarek, 2017; Sajil Kumar et al., 2014). The interrelationship between various ions will demonstrate the different rock-water interactions occurring in the aquifer. Geochemical modelling using PHREEQC code is being used

* Corresponding author.

E-mail address: klpriyaram@gmail.com (K.L. Priya).<https://doi.org/10.1016/j.gsd.2020.100393>

Received 24 April 2019; Received in revised form 26 January 2020; Accepted 9 April 2020

Available online 17 April 2020

2352-801X/© 2020 Elsevier B.V. All rights reserved.

geochemical processes in the aquifer using the above mentioned state-of-the-art techniques is found lacking in literatures as far as the aquifers of Coimbatore is concerned. This study is therefore aimed at investigating the major hydrogeochemical processes occurring in the aquifer system of Coimbatore city, Tamil Nadu. The main objective was to identify the different mechanisms controlling groundwater chemistry through a systematic study of the geochemical and geospatial techniques. The study specifically explored the role of textile mills on the geochemical processes in the aquifer. As the groundwater forms the major source for irrigation, an evaluation of its suitability for irrigation was carried out.

2. Study area

2.1. General

The Coimbatore city, the administrative headquarters of Coimbatore district is one of the highly industrialized city in South India (Fig. 1). Located between $10^{\circ} 55' - 11^{\circ} 10'N$ latitude and $76^{\circ} 50' - 77^{\circ} 10'E$ longitude, it is surrounded by the western ghats to the North & West and have an elevation of ca. 430 m above M.S.L. The topography of the city slopes from North towards South and from West towards East (Fig. 2). Noyyal river, a tributary of Cauvery river runs through Coimbatore and forms the southern boundary of the city (Fig. 2). The city is known for its textile factories and is often referred to as the Manchester of South India. In 1888, the first textile mill started and since then, there are over 100 mills in operation. Moreover, there are more than 25,000 small to large scale industries in Coimbatore, thereby forming a major economy driving force for Tamil Nadu (MSME, 2013). Thus, the land use of Coimbatore is mainly consisting of built up land except at the banks of Noyyal river, where most of the land is occupied by agricultural field.

2.2. Hydrological setting

The climate is generally tropical with lowest temperature during November to February ($\approx 17^{\circ}C$) and highest temperature during March to May ($\approx 39^{\circ}C$). The average annual rainfall varies from 550 mm to 900 mm under the influence of North-East and South-West monsoons. The northeast monsoon occurs during October–November months, which contributes to the major portion of rainfall in the city and summer rains are negligible. The period from April to June is generally hot and dry and consists of summer. Fig. 3 represents a typical rainfall histogram for the study area. This rainfall is not sufficient to sustain the demand of the city for the entire year and the shortage is partially covered through water supply schemes like Siruvani, Pillor and Athikkadavu. The

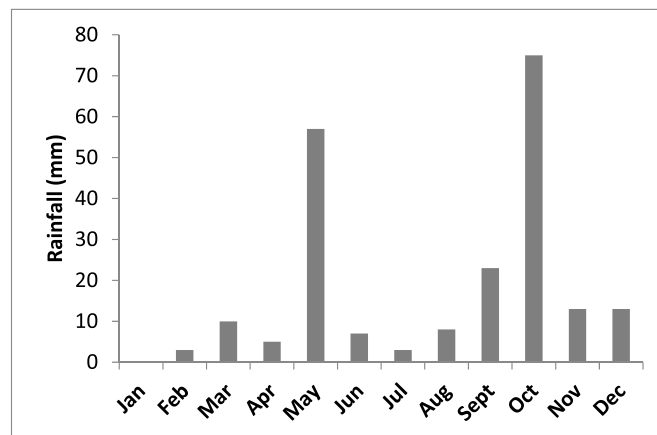


Fig. 3. Rainfall distribution in Coimbatore.

remaining demand is being fulfilled by water extracted from the aquifer through dug and bore wells.

The city is located in the Noyyal river basin, a sub-basin of Cauvery river basin. The Noyyal is a seasonal river having good flow only during the North-East and South-West monsoon. The river emerges in the Vellangiri hills of the Western Ghats and flows over a distance of 180 km in an area of 3510 sq. km to join Cauvery river at Karur district. There are 8 major wetlands Singanallur, Velankulam, Ukkadam Periyakulam, Selvampathi, Narasampathi, Krishnampathi, Selvachinthamani and Kumaraswami, fed by the Noyyal river and are mostly used for irrigation purposes. Some of the natural drains in the city include Sanganur palam, Velangurichi-Singanallur drain, Railway feeder road-side drain, Trichy-Singanallur check drain, Ganapathy drain, Koilmedu drain and Karperayam koil drain.

2.3. Geological setting

Geology of Coimbatore is mainly characterized by the peninsular gneiss complex and the local rock formation can be classified as a wide range of metamorphic rocks, which are extensively weathered and overlain by recent valley fills and alluvium. The geological formations found in the district are.

Khondalite, Calc-granulite, complex gneiss mainly Hornblende-Biotite and crystalline limestone, Dolerite, Charnockite, Granite gneiss, Granite and Syenite, Pegmatite, and Quartzite veins. Fissured granitic gneiss and massive granitic gneiss form the bed rocks. Table 1

Table 1 Geological details and the components.

Type of Rock	Main components
Khondalite	Quartz-manganese-rich garnet-rhodnite schist
Complex gneiss	Hornblende ((Ca, Na) ₂₋₃ (Mg,Fe,Al) ₅ (Al,Si) ₈ O ₂₂ (OH,F) ₂) Biotite (K(Mg,Fe) ₃ (AlSi ₃ O ₁₀)(F,OH) ₂)
Pink granite	Quartz (SiO ₄) Feldspar (KAlSi ₃ O ₈ -NaAlSi ₃ O ₈ - CaAl ₂ Si ₂ O ₈) Hornblende ((Ca, Na) ₂₋₃ (Mg,Fe,Al) ₅ (Al,Si) ₈ O ₂₂ (OH,F) ₂) Lepidolite (K(Li,Al,Rb) ₃ (Al,Si) ₄ O ₁₀ (F,OH) ₂) Sillimanite Gneiss (Al ₂ SiO ₅)
Charnockite	Orthopyroxene (Ca,Mg,Fe) ₂ Si ₂ O ₆ Quartz (SiO ₄) Feldspar (KAlSi ₃ O ₈ -NaAlSi ₃ O ₈ - CaAl ₂ Si ₂ O ₈)
Limestone	Calcite and aragonite (CaCO ₃)
Dolomite	CaMg(CO ₃) ₂
Quartz pegmatite	Quartz (SiO ₄) Feldspar (KAlSi ₃ O ₈ -NaAlSi ₃ O ₈ - CaAl ₂ Si ₂ O ₈) Mica
Calc-granulite	Calcite (CaCO ₃) Hornblende ((Ca, Na) ₂₋₃ (Mg,Fe,Al) ₅ (Al,Si) ₈ O ₂₂ (OH,F) ₂)
Syenite	Feldspar (KAlSi ₃ O ₈ -NaAlSi ₃ O ₈ - CaAl ₂ Si ₂ O ₈)

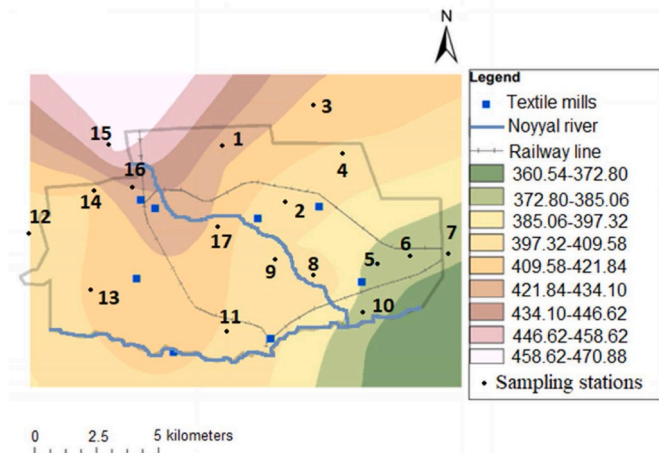


Fig. 2. Map showing topography, textile mills and Noyyal river and location of sampling stations.

shows the various components of rocks of the study area. Coimbatore is the source of many mineral resources namely gypsum, feldspar, limestone and quartz/silica, magnesite (Source: Department of Mines & Geology, Coimbatore).

The four major types of soil in the study area include black cotton soil (9.14%), reddish brown/brown loamy soil (4.86%), alluvium and colluvium (8.91%), red calcareous soil (63.83%) and red non-calcareous soil (13.26%) (Subburaj, 2008). The main constituent of soil in the study area is CaCO_3 due to the predominance of red calcareous soil. Kankar is followed by top soil at certain areas. The sand deposit is predominant at the eastern side. Fig. 4 represents the soil in the district.

2.4. Hydrogeological setting

In Coimbatore, groundwater occurs in all geological formations from the oldest archaen to recent alluvium. The geological formation, lithological variation, tectonic complexity and geomorphological and hydrometeorological dissimilarities existing in the region give rise to a variety of groundwater situations. Based on the mode of occurrence, the hydrogeological framework has been divided into two categories: fissured and fractured formation, both in gneiss and charnockite formation and porous formation (Fig. 5). The porous formation in the area is represented by alluvium, colluvium and laterites. The groundwater in the region with colluvium formation occurs under phreatic conditions in the aquifer at depth ranging from 30 to 60 m. In alluvium formation, consisting mainly of silt and clay, groundwater occurs under water table conditions or semi-confined and the formations are highly porous, permeable and developed into potential water bearing zones. The depth to water level depends on the rainfall intensity and is variable over the year. The water is produced by the usage of dug wells and bore wells.

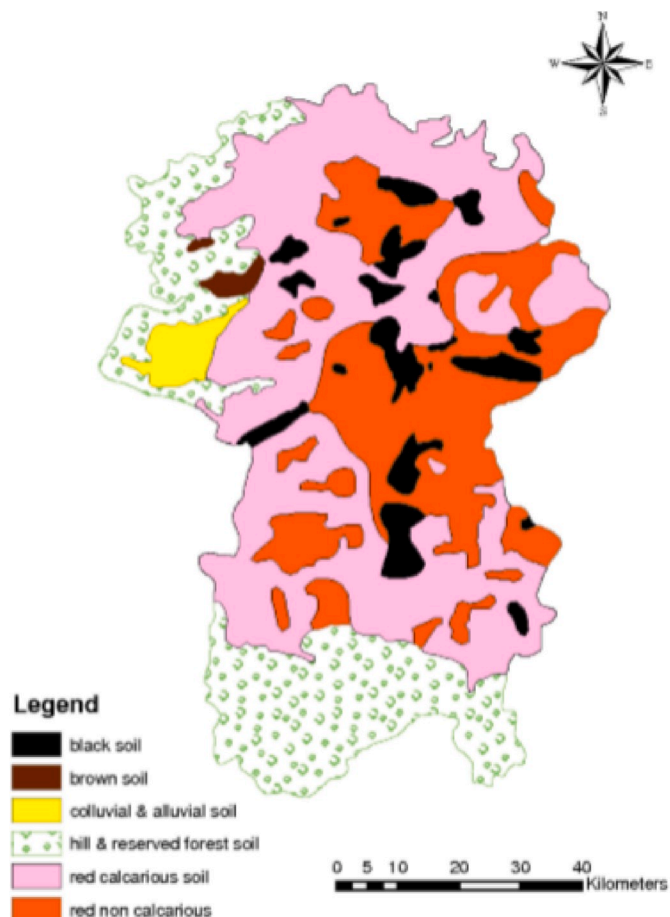


Fig. 4. Soil map of Coimbatore district (Source Kumar and Aneesh, 2012).

3. Materials and methods

3.1. Groundwater sampling and analysis

Groundwater samples were collected from 17 wells during the post-monsoon (October 2015) and the pre-monsoon (April 2015) seasons (Fig. 2). The samples were collected in polyethylene bottles pre-cleaned with de-ionized water. The bottles were rinsed using the groundwater samples before collection. For determining each parameter of each sample, three replicates were carried out. The parameters such as pH, electrical conductivity (EC), total dissolved solids (TDS) and temperature were measured in-situ using a portable water quality analyser (Systronics Water Analyser 371) after proper calibration. The collected samples were transferred to the laboratory and were analysed for the major cations such as Ca^{2+} , Mg^{2+} , Na^+ , K^+ and major anions such as Cl^- , SO_4^{2-} , HCO_3^- and CO_3^{2-} and for total hardness as per APHA, (1998) standard methods. The Ca^{2+} and Mg^{2+} were analysed using titrimetric methods using standard EDTA. Na^+ and K^+ were determined using flame photometer. Cl^- was analysed by argentometric method by titration with AgNO_3 ; HCO_3^- and CO_3^{2-} were determined by acid titration and SO_4^{2-} by spectrophotometry. Fluoride concentration was found using spectrophotometer using SPANDS reagent.

For the analysis of heavy metals, the samples were collected in bottles pre-cleaned by soaking in detergent followed by soaking in 10% nitric acid for 48 h and finally rinsed with deionized water. The samples were filtered and acid stabilized soon after collection. Metal ion concentrations were determined by atomic absorption spectrometer (Model 3110) using air-acetylene flame. Quantification of metals was based upon calibration curves of standard solution of respective metals. The detection limits for Fe, Mn, Cu, Ni, Cr, Pb, Cd and Zn are 0.003, 0.001, 0.004, 0.002, 0.01, 0.0005, 0.0008 and 0.004 mg/L respectively.

The suitability of groundwater for irrigation purposes was assessed using salinity hazard, alkalinity hazard, % Sodium, permeability index, magnesium ratio and kelly ratio. Hydrochemical classification was done using Piper diagram and the various hydrogeochemical facies existing in the study area were identified. Hydrochemical evolution of groundwater was delineated using Gibbs diagram and the influence of rock-water interaction, evaporation and precipitation on the groundwater chemistry was studied. The mutual relationships existing between the major cations and anions were investigated through $\text{Ca}^{2+}/\text{Mg}^{2+}$ ratio, $(\text{Ca}^{2+} + \text{Mg}^{2+})/(\text{HCO}_3^- + \text{SO}_4^{2-})$ ratio, $(\text{Na}^+ + \text{K}^+)/\text{total cations}$ ratio, $(\text{Ca}^{2+} + \text{Mg}^{2+})$ vs EC plot, Na^+/Cl^- vs EC plot and chloroalkaline indices and the analysis lead to the identification of the processes controlling the groundwater chemistry. Further, geochemical modelling was attempted using the geochemical code PHREEQC to analyse the degree of equilibrium between water and minerals in the aquifer.

4. Results and discussion

4.1. General chemistry

The summary of statistics of qualitative parameters of groundwater samples during the post-monsoon and pre-monsoon is presented in Table 2. The groundwater was slightly alkaline in nature with the pH varying between 7.1 and 7.6 during the post-monsoon and between 7 and 7.8 during the pre-monsoon. A wide spatial and temporal variation in electrical conductivity (EC) was observed in the study area. The range of EC was between 532 and 6240 $\mu\text{S}/\text{cm}$ and between 300 and 8360 $\mu\text{S}/\text{cm}$ during the post-monsoon and pre-monsoon respectively and the corresponding variations of TDS was 340–3934 mg/L and 192–5451 mg/L 82% of the samples are classified as brackish (Total Dissolved Solids (TDS) of 1000–10,000 mg/L) with the remaining samples falling under freshwater category (250–1000 mg/L) as per the classification proposed by Todd (1980). 88% of the samples fall under very hard category (>300 mg/L) based on the classification system proposed by Sawyer and McCarty (1967) with the total hardness ranging between

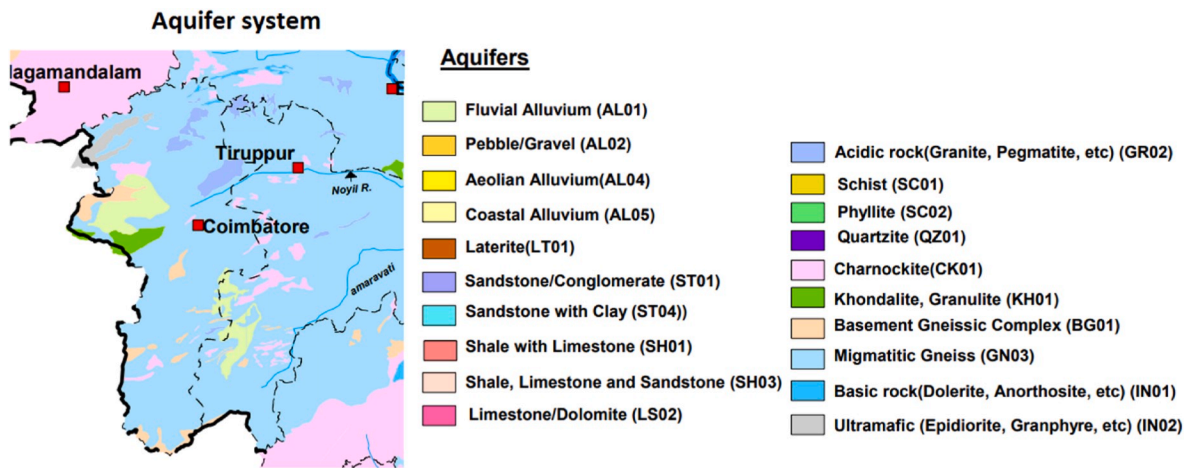


Fig. 5. Hydrogeology map of Coimbatore district (Source: Central Groundwater Board, MoWR, GoI).

Table 2
Statistical summary of qualitative analysis of the groundwater.

Parameter	Maximum		Minimum		Mean		Standard Deviation	
	Post-M	Pre-M	Post-M	Pre-M	Post-M	Pre-M	Post-M	Pre-M
pH	7.6	7.8	7.1	7.0	7.4	7.5	0.15	0.24
Electrical Conductivity, $\mu\text{S}/\text{cm}$	6240	8360	532	300	3078	3095	1750	1893
Total Dissolved Solids, mg/L	3934	5451	340	192	1874	1989	1104	1233
Total Hardness, mg/L	1425	3400	279	230	820	894	417	756
Ca^{2+} , mg/L	451	318	30	135	175	202	137	43
Mg^{2+} , mg/L	243	160	22	12	100	70	56	41
Na^+ , mg/L	380	823	32	95	186	349	117	197
K^+ , mg/L	87	182	4	6	28	27	27	41
Cl^- , mg/L	1614	1500	28	44	532	552	494	479
$\text{CO}_3^{2-} + \text{HCO}_3^-$, mg/L	561	600	146	336	430	490	104	79
SO_4^{2-} , mg/L	880	166	25	14	178	56	250	44
F^- , mg/L	1.8	1.28	0.21	0	0.88	0.46	0.42	0.49
Fe, $\mu\text{g}/\text{L}$	570	455	90	8	252	103	136	113
Mn, $\mu\text{g}/\text{L}$	52	55	9	4	30	32	14	16
Zn, $\mu\text{g}/\text{L}$	480	1067	5	0	82	176	121	316
Cr, $\mu\text{g}/\text{L}$	70	73	0	0	16	14	23	21
Cu, $\mu\text{g}/\text{L}$	13	10	0	0	1.6	0.7	3.2	2.4
Ni, $\mu\text{g}/\text{L}$	148	145	30	4	74	66	31	42
Pb, $\mu\text{g}/\text{L}$	70	6	0	0	16	1	23	2

279 & 1425 mg/L during the post-monsoon and between 230 and 3400 mg/L during the pre-monsoon. The results show that the groundwater is highly mineralized in the study area.

The dominance of major cations in the groundwater samples followed the order $\text{Ca}^{2+} > \text{Na}^+ > \text{Mg}^{2+} > \text{K}^+$ (meq/L) while the major anions followed the order $\text{Cl}^- > \text{HCO}_3^- + \text{CO}_3^{2-} > \text{SO}_4^{2-}$ (meq/L) during both the seasons. The ion balance errors of all the samples during both the seasons were within $\pm 5\%$. The concentration of Ca^{2+} ranged between 30 and 451 mg/L during the post-monsoon and between 135 and 318 mg/L during the pre-monsoon, while the range of Mg^{2+} was 22–243 mg/L and 12–160 mg/L during the post-monsoon and pre-monsoon respectively. These ions may be derived from calcium and magnesium bearing rocks namely charnokite, granite and gneiss. The concentration of Na^+ and K^+ ranged respectively from 32 to 380 mg/L and from 4 to 87 mg/L during the post-monsoon and from 95 to 823 mg/L and 6–182 mg/L during the pre-monsoon. A higher concentration of Ca^{2+} ions among the cations may be attributed to rock weathering or dissolution of soil minerals. Another cause of dominance of alkali earth elements over alkali elements may be the ion exchange process between rock and water.

The variation of Cl^- was between 28 & 1614 mg/L during the post-monsoon and between 44 & 1500 mg/L during the pre-monsoon. Weathering and dissolution of salt deposits, percolation from

agricultural fields and discharge from industrial wastewater are some of the common causes of higher chloride content in groundwater (Jeevanandam et al., 2012). Higher carbonate and bicarbonate concentrations leading to alkalinity of water was observed in the study area with their concentration varying between 146 & 561 mg/L during the post-monsoon and between 336 & 600 mg/L during the pre-monsoon. They are probably derived from the weathering of limestone, dissolution of carbonate precipitates, atmospheric and soil carbon-di-oxide (Jeong, 2001). The least dominant anion in the groundwater was sulphates and it ranged between 25 and 880 mg/L during the post-monsoon and between 14 and 166 mg/L during the pre-monsoon. Contamination from industrial and domestic sewage are likely to cause an increase in the concentration of sulphates (Baruah et al., 2008) at some locations. A marginally higher concentration of fluorides was observed for 35% and 18% of the samples with its value peaking to 1.8 and 1.28 mg/L during the post-monsoon and pre-monsoon respectively. Biotite, hornblende, lepidolite and mica are the major components of rocks contributing to fluorides in groundwater. Some of the major factors that affect the dissolution of fluoride from rocks in groundwater include pH, temperature, anion exchange capacity, residence time, depth, age of groundwater, concentration of carbonates and bicarbonates (Apambire et al., 1997).

Over 24% of the samples exhibited a Fe concentration greater than

BIS drinking water standards of 300 µg/L with its values ranging between 90 & 570 µg/L during the post-monsoon and 8 & 455 µg/L during the pre-monsoon. Biotite and hornblende are the major sources of Fe in the study area and it is expected that conditions favorable for the reduction of ferric ion into ferrous ion exists in the location. It was observed that all the samples exhibited low concentration of Mn, Zn and Cu during both the seasons and were well below the BIS drinking water standards of 100 µg/L, 5000 µg/L and 50 µg/L respectively. Cd was below the detection limits in all the samples (hence not given in Table 2). Except 12% of the samples during the post-monsoon and 1% during the pre-monsoon, Cr concentration in all the samples were within BIS drinking water standards of 50 µg/L. Nevertheless, all the samples had Ni concentrations exceeding the BIS standards of 20 µg/L during both the seasons. The health effects due to exposure to Nickel include nausea, headache, vomiting, skin irritation, hypersensitivity and carcinogenicity. Nickel is extensively used in textile mills, where they use nickel phthalocyanines (bright green dyes) during the dyeing process. A number of textile mills are located in the study area as can be seen from Fig. 2. The wastewater from the textile mills are discharged into the Noyyal river, which ultimately reaches the groundwater table. The mobility of Nickel is enhanced by the presence of Fe and Mn oxides in the aquifer. While biotite and hornblende contribute to Fe, Mn may be contributed by khondalite. It was observed that there was a good correlation of Fe and Mn with Ni during the post-monsoon (Table 3). This suggests that when the groundwater flow is appreciable, Ni is highly mobilized in the aquifer, causing a wide spread distribution, even though the dilution effect of rain plays a role to reduce the concentration (Fig. 6). During the pre-monsoon, the concentration of Ni is marginally high because of the absence of dilution effect and this leads to the distribution of Ni on the central and south-eastern regions (Fig. 6). Salt is extensively used during the dyeing process. There was a consistent positive correlation of Ni with EC and TDS (Table 4) during both the seasons. Further, the spatial variation of Ni (Fig. 6) and TDS (Fig. 7) show that both Ni and TDS have higher concentration at same spatial areas, thereby depicting that Ni and TDS are arrived from the same source. Also, referring the location of textile mills (Fig. 2), it is certain that textile mills can be the possible source of contamination of groundwater in the central and south-eastern regions. It is interesting to note that the distribution of Ni resembles the topography of Coimbatore (Fig. 2), suggesting that the tributary of Noyyal river (see Fig. 2), which carries the wastewater, recharges the groundwater and therefore spatial distribution of Ni follows that of the flow pattern in the aquifer i.e. from north-western to south-eastern direction. Thus, textile mills can be considered as the possible contributors of Nickel in the groundwater of Coimbatore.

Around 41% of the samples during post-monsoon exhibited Pb

Table 3
Correlation among heavy metals during post-monsoon and pre-monsoon.

Post-M	Fe	Mn	Zn	Cr	Cu	Ni	Pb
Fe	1						
Mn	0.56	1					
Zn	0.00	-0.28	1				
Cr	0.37	0.58	-0.07	1			
Cu	-0.01	-0.30	0.70	-0.34	1		
Ni	0.83	0.72	-0.15	0.45	-0.07	1	
Pb	0.39	0.56	-0.07	0.99	-0.33	0.50	1
Pre-M	Fe	Mn	Zn	Cr	Cu	Ni	Pb
Fe	1						
Mn	0.07	1					
Zn	-0.21	-0.36	1				
Cr	-0.23	0.22	0.12	1			
Cu	0.15	-0.28	-0.11	0.25	1		
Ni	-0.08	0.14	-0.07	0.19	-0.07	1	
Pb	0.64	-0.17	0.09	-0.20	0.01	-0.01	1

Note: bold value shows significant at 0.05 level.

concentrations exceeding BIS standards (10 µg/L); the maximum reported concentration being 70 µg/L. On the other hand, the concentration of Pb during the pre-monsoon was well within the permissible limit in all the samples. Pb is primarily used in the production of lead-acid batteries, solder and alloys. The various effects due to exposure to lead include neuro developmental effects, mortality due to cardiovascular diseases, impaired renal function, hypertension and impaired fertility (WHO, 2017).

Correlation analysis reveals that Pb is having high positive correlation with Fe thereby suggesting the association of Pb with Fe (Table 3). Pb is likely mobilized in groundwater through adsorptive retardation by iron oxy hydroxides. Further, the high correlation of Pb with Cr indicates that both are originated from the same source. They are possibly transported by percolation through the precipitation during the post-monsoon. During the pre-monsoon, ion exchange of Pb with Ca of calcite may have probably lead to the reduction of Pb in groundwater, thereby increasing the concentration of Ca in groundwater, as evidenced by the higher concentration of Ca in the samples during pre-monsoon.

4.2. Hydrogeochemical classification

4.2.1. Classification of water for irrigation

Groundwater is the major source of water for irrigation accounting for 92% of the total irrigated area in Coimbatore district. Being the dominant source of water for irrigation, an analysis of the suitability of groundwater for irrigation purposes was carried out. The major parameters that are important for irrigation water include salinity hazard (Electrical Conductivity), Alkalinity hazard (Sodium Absorption Ratio SAR) Percentage Sodium (% Na), permeability index (PI), Magnesium ratio (MR) and Kelly ratio (KI). Table 5 gives the different classification systems generally adopted for classifying irrigation water and the % of samples falling under in each category from the study area.

SAR is the ratio between Na^+ and $\text{Ca}^{2+} + \text{Mg}^{2+}$ ions and is a measure of alkali/sodium hazard to crops (Subramani et al., 2010). Higher amounts of Na^+ relative to Ca^{2+} and Mg^{2+} ions can cause dispersion of soil colloids, thereby destroying soil texture and permeability (Kumar et al., 2007).

The US Salinity Laboratory classification system classify irrigation water into 4 categories based on SAR and EC: Excellent ($\text{SAR} < 10$ & $\text{EC} < 250$ µS/cm); Good ($\text{SAR}: 10-18$ & $\text{EC}: 250-750$ µS/cm); Satisfactory ($\text{SAR}: 18-26$ & $\text{EC}: 750-2250$ µS/cm); Bad ($\text{SAR} > 26$ & $\text{EC} > 2250$ µS/cm) (Richards, 1954). The salinity hazard and alkalinity hazard of groundwater samples can be best represented by Wilcox diagram (Wilcox, 1955). As per the classification, 12% of the samples fall under S3C4 category, 37% of the samples under S2C4 category and the remaining samples can be categorized as S1C3 and S1C2 (Fig. 8).

Sodium interacts with soil and reduces its permeability (Parthasarathy et al., 2012) through adsorption on to clay particles followed by ion exchange with Ca^{2+} and Mg^{2+} ions from the soil. As a result, internal drainage is lowered leading to reduced circulation of air and water and ultimately the soil becomes hard (Saleh et al., 1999). Wilcox (1955) put forward a method for classifying irrigation water based on sodium percentage, accordingly 12% of the samples fall under excellent category with a %Na < 20 and the remaining under good and permissible category during the post-monsoon, while 23% of the samples had a % Na > 60 during the pre-monsoon showing that the water samples are not satisfactory for irrigation (Table 5).

A criteria for assessing the irrigation water was proposed by Doneen (1964) on the basis of the influence of Na^+ , Ca^{2+} , Mg^{2+} and HCO_3^- on the permeability of soil. According to him, the permeability index is the ratio of $(\text{Na}^+ + \text{HCO}_3^-)$ to $(\text{Ca}^{2+} + \text{Mg}^{2+} + \text{Na}^+)$. A permeability index of >75% is classified as Class I and between 25% and 75% as Class II and are suitable for irrigation, while if the index is <25% the water is unsuitable for irrigation. All the samples from the study area fall either under Class I or Class II, thereby indicating their suitability for irrigation. Considering the ratio of Na^+ to $\text{Ca}^{2+} + \text{Mg}^{2+}$, which is defined as

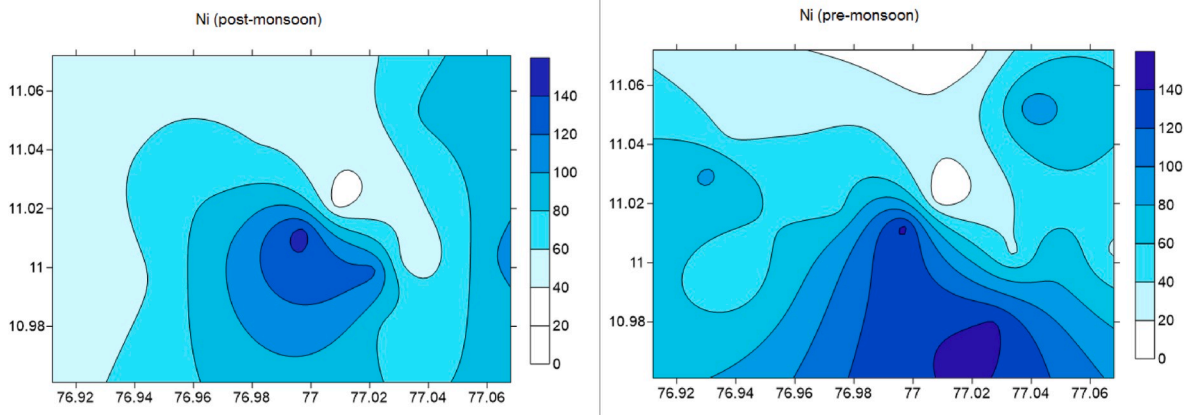


Fig. 6. Spatial map showing the distribution of Nickel in the study area.

Table 4

Correlation of Nickel with chemical parameters during post-monsoon and pre-monsoon.

Parameter	Post-monsoon	Pre-monsoon
pH	-0.56	-0.26
EC	0.66	0.65
TDS	0.67	0.64
Ca ²⁺	0.28	0.09
Mg ²⁺	0.75	0.55
Na ⁺	0.66	0.34
K ⁺	0.81	0.08
Cl ⁻	0.67	0.53
HCO ₃ ⁻	-0.2	0.2
SO ₄ ²⁻	0.52	-0.36
F ⁻	0.28	-0.48

Note: bold value shows significant at 0.05 level.

Kelly ratio (Kelley, 1951), all the samples exhibited a value < 1 and are suitable for irrigation during the post-monsoon; 35% of the samples were found to be unsuitable for irrigation during the pre-monsoon.

In natural waters, Ca²⁺ and Mg²⁺ ions will be in equilibrium (Hem, 1989). However, some of the processes such as ion exchange and rock-water interaction may disrupt the equilibrium leading to high Mg²⁺ ions in water, which can have adverse effects on the yield of crop when used for irrigation (Kumar et al., 2007). The Mg ratio is calculated as the ratio of Mg²⁺ to the sum of Ca²⁺ and Mg²⁺ (Paliwal, 1972):. A Mg ratio of <50% is considered as suitable for irrigation and comprises of 41% and 82% of the samples during post-monsoon and pre-monsoon respectively.

4.2.2. Hydrochemical facies

The groundwater chemistry is governed by geochemical reactions occurring in the aquifer or by the intrusion followed by contamination from neighbourhood areas. The various geochemical compositions arising from these processes can be identified by analyzing the hydro-geochemical facies of groundwater using Piper diagram (Piper, 1944). The diagram consists of two triangular and a central diamond shaped field and from the position of the water sample in the field, the water type can be identified (Fig. 9). The diagram reveals that alkaline earths (Ca²⁺ & Mg²⁺) exceed alkalis (Na⁺ & K⁺) and strong acids (Cl⁻ & SO₄²⁻) exceed weak acids (HCO₃⁻ & CO₃²⁻) during both the seasons for majority of the samples. However, for a small group of samples, the phenomenon was reversed during the transition from post-monsoon to pre-monsoon. 57% of the samples fall under mixed Ca-Mg-Cl type while 35% fall under Ca, Mg-HCO₃ type during the post-monsoon. Some of the samples which exhibited Ca-type were converted to Na-type or mixed Ca,Na-type during the transition from post-monsoon to pre-monsoon, and that accounted for 29% of the samples. The samples on the central part exhibited this transition (Fig. 10). This has occurred mainly at locations of textile mills (Fig. 2). It is suspected that the textile mills are a main contributor to the water type in the central regions. The chemicals used by the textile mills during the scouring (caustic soda, soda ash), mercerizing (caustic soda), bleaching (sodium hypochlorite) and dyeing process are released into the Noyyal river, and subsequently reach the groundwater table. It can be noted that Na⁺ ions are the major cations in all these chemicals used. During post-monsoon, the rainwater dilute the concentration of textile wastewater in the river, thereby reducing the concentration of Na⁺ ions and thus the Ca²⁺ ions dominate Na⁺ ions,

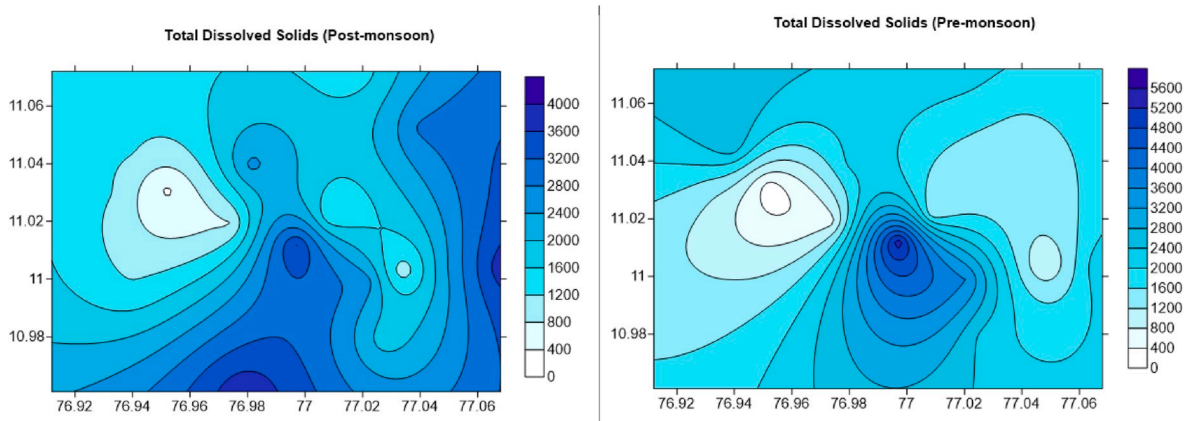


Fig. 7. Spatial map showing the distribution of Total Dissolved Solids in the study area.

Table 5
Classification of water for irrigation.

Classification System proposed by	Classification parameters	Range	Category	% of samples	
				Post-monsoon	Pre-monsoon
USSL (Richards, 1954)	Salinity hazard (EC $\mu\text{S}/\text{cm}$)	<250	Excellent	0	0
		250–750	Good	6	6
		750–2250	Doubtful	41	35
		>2250	Unsuitable	53	59
	Alkali hazard (SAR)	<10	Excellent	100	94
		10–18	Good	0	6
		18–26	Doubtful	0	0
		>26	Unsuitable	0	0
Wilcox, (1955)	% Sodium	<20	Excellent	12	0
		20–40	Good	82	24
		40–60	Permissible	6	53
		60–80	Doubtful	0	23
		>80	Unsuitable	0	0
Doneen, (1964)	Permeability Index	>75%	Excellent	35	47
		75–25%	Permissible	65	53
		<25%	Unsuitable	0	0
Kelley, 1951	Kelly ratio	<1	Suitable	100	65
		>1	Unsuitable	0	35
		>1	Unsuitable	71	65
Paliwal, 1972	Magnesium hazard	<50%	Suitable	41	82
		>50%	Unsuitable	59	18

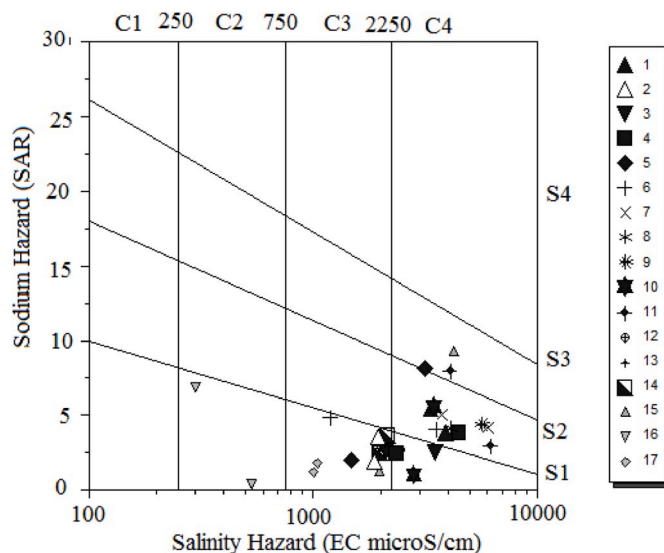


Fig. 8. Water classification based on SAR and EC (after Wilcox, 1955).

resulting in the Ca-type of water. Nevertheless, during the pre-monsoon, in the absence of rainfall, there will be higher degree of concentration of Na^+ in the river, thereby increasing the levels of Na^+ ions in comparison with Ca^{2+} ions. Thus, textile mills contribute to the water type of the central and south-eastern regions of the study area wherein Ca-type during post-monsoon was converted to Na-type or mixed Ca,Na-type during the pre-monsoon. Thus, the contamination from textile mills has caused a seasonal variability in the aquifer characteristics, especially the water type.

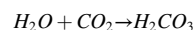
4.3. Hydrochemical evolution

In order to further delineate the processes controlling groundwater chemistry, Gibbs diagram proposed by Gibbs (1970) was plotted. It is used to interpret the influence of rock-water interaction, evaporation and precipitation on the groundwater chemistry. The Gibbs ratios are plotted against TDS concentrations as shown in Fig. 11. The cation ratio varied from 0.06 to 0.76 and the anion ratio between 0.16 and 0.85. Most of the samples fall under rock-water interaction and

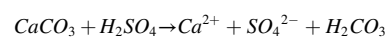
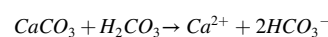
evaporation-crystallization dominant zone. The rock-water interactions that affect the groundwater chemistry include chemical weathering of rocks, dissolution/precipitation of secondary carbonates and ion exchange between water and clay minerals. The samples falling under evaporation zone exhibit higher Cl^- ions and consequently higher TDS concentrations. As the phenomenon of evaporation is not much predominant in the deep aquifers as in the study area, the high TDS may be attributed to contamination from anthropogenic activities especially from textile mills, as described earlier. Hence, evaporation may not have much influence on the groundwater chemistry.

4.4. Hydrochemical relations

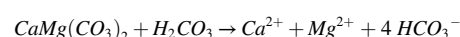
An analysis of the relationship among major ions is essential for understanding the natural rock-water interaction process taking place in the aquifer. The dominant cations in most of the samples include Ca^{2+} and Mg^{2+} . Calcite and aragonite are the predominant rocks rich in Ca^{2+} while the presence of Ca^{2+} and Mg^{2+} in groundwater may be due to weathering of dolomite. The weathering of dolomite rocks will be predominant at locations with a $\text{Ca}^{2+}/\text{Mg}^{2+}$ molar ratio <1 (Mayo and Loucks, 1995), while a $\text{Ca}^{2+}/\text{Mg}^{2+}$ ratio between 1 and 2 represents calcite weathering and a greater $\text{Ca}^{2+}/\text{Mg}^{2+}$ ratio indicate silicate weathering (Katz et al., 1997). 65% of the samples exhibited a $\text{Ca}^{2+}/\text{Mg}^{2+}$ ratio <1, 18% between 1 and 2 and 17% had ratios >2 during the post-monsoon while 17% of the samples showed a ratio <1, 29% between 1 and 2 and over 53% of the samples have $\text{Ca}^{2+}/\text{Mg}^{2+}$ ratio >2. The dissolution of rocks is driven by the presence of CO_2 in the aquifer, which is liberated during the degradation of organic matter present in the soil. The fundamental process to weathering includes:



Carbonate rocks (limestone rocks) such as calcite, aragonite and dolomite undergo dissolution under natural conditions as given below:
Calcite and Aragonite:



Dolomite:



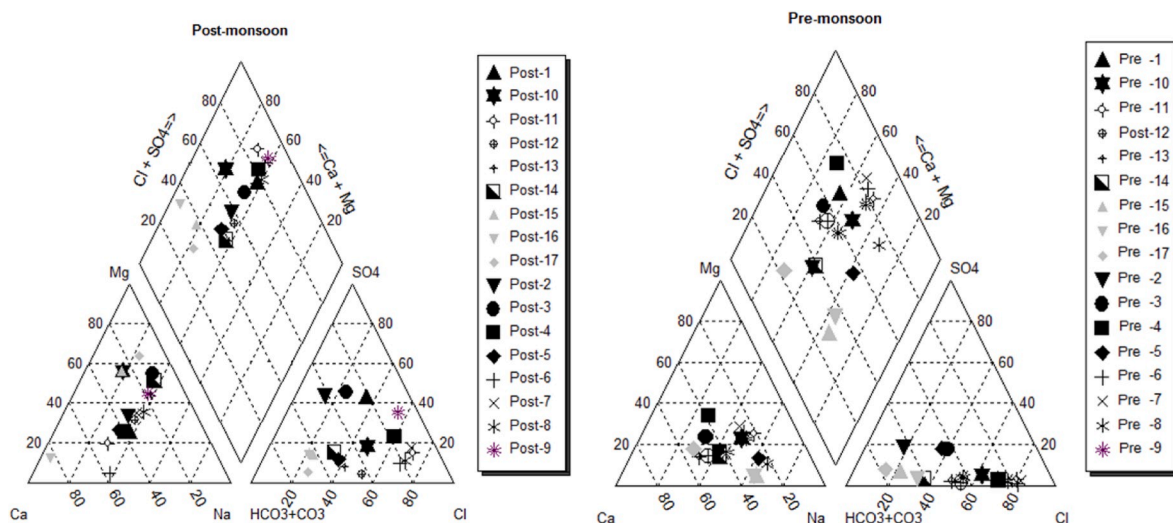


Fig. 9. Piper diagram representing hydrogeochemical facies of groundwater in the study area during the post-monsoon and the pre-monsoon.

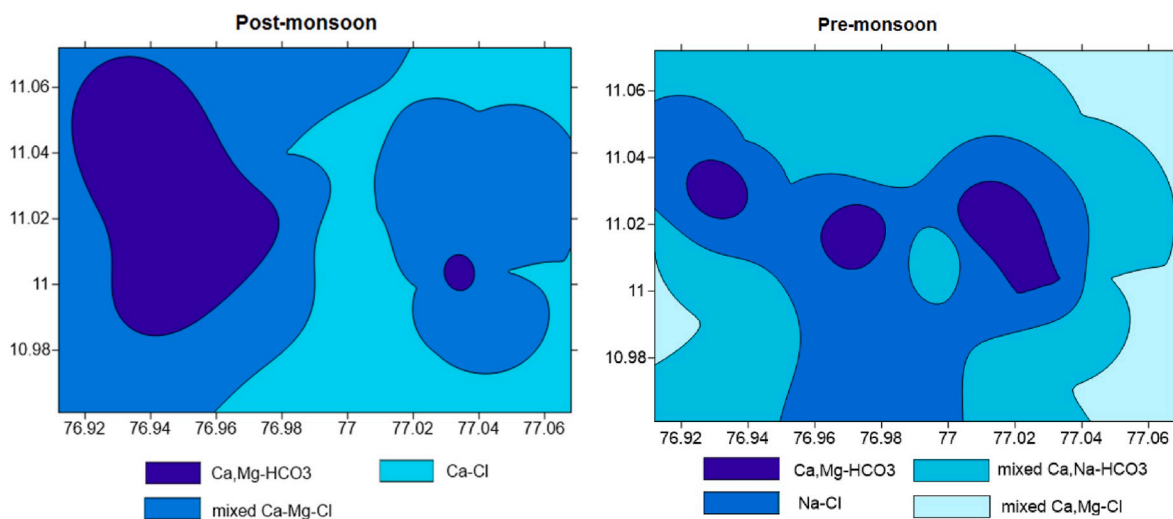
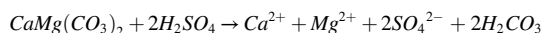
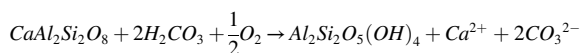


Fig. 10. Spatial map showing hydrochemical facies of groundwater during post-monsoon and pre-monsoon.

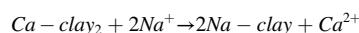


Another dominant mineral in the study area is feldspar of granite rocks. It may undergo hydrolysis and get altered to clay minerals releasing Ca^{2+} as depicted below:

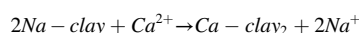


A higher Ca^{2+}/Mg^{2+} ratio was exhibited in the north-western regions (Fig. 12) where the water was of Ca, Mg-HCO₃ type. The results suggest that carbonate weathering predominate in those regions of the study area. The huge deposits of limestone may be the source for carbonate weathering. In addition, the red calcareous soil may also contribute to carbonate leading to the release of Ca^{2+} ions to water. The dominance of carbonate weathering is suspected when Ca^{2+} & Mg^{2+} dominate HCO_3^- and SO_4^{2-} , resulting in an increase in Ca^{2+} and Mg^{2+} in groundwater (Elango and Kannan, 2007). The plot between $Ca^{2+} + Mg^{2+}$ and $HCO_3^- + SO_4^{2-}$ will be near 1:1 equiline if Ca^{2+} , Mg^{2+} , SO_4^{2-} and HCO_3^- are derived from calcite, aragonite, dolomite and gypsum. The average $(Ca^{2+} + Mg^{2+}) / (HCO_3^- + SO_4^{2-})$ was greater than 1 (1.7) with the ratios ranging between 0.6 and 2.3 (Fig. 13(a)). 23% of the samples were clustered near 1:1 equiline, indicating that the dissolution of calcite, dolomite and aragonite lead to higher Ca^{2+} & Mg^{2+} in groundwater.

Majority of the samples are shifted to the left of the equiline and have an excess of $Ca^{2+} + Mg^{2+}$ and may be dominated by ion exchange process, wherein Na^+ in water is exchanged for Ca^{2+} from clay, which is seen in alluvium formations, as indicated below:



The Na^+ in water is possibly contributed by the textile mill effluents, where salt and caustic soda are used for dyeing, scouring, bleaching and mercerizing process and are generally discharged without proper treatment. This suggest that the contamination from textile mills through the release of Na^+ into the aquifer enhances the ion exchange process, thereby leading to an increase in the concentration of Ca^+ ions in the aquifer. 17% of the samples fall below the 1:1 equiline during the post-monsoon and are shifted to the right of the 1:1 equiline have an excess of $SO_4^{2-} + HCO_3^-$, which can be attributed to reverse ion exchange process as shown below:



In addition to carbonate weathering, weathering of silicates can play a major role in controlling the hydrogeochemistry of groundwater (Garrels and Mackenzie, 1967). The ratio between $Na^+ + K^+$ and total cations is generally considered for identifying the process of silicate

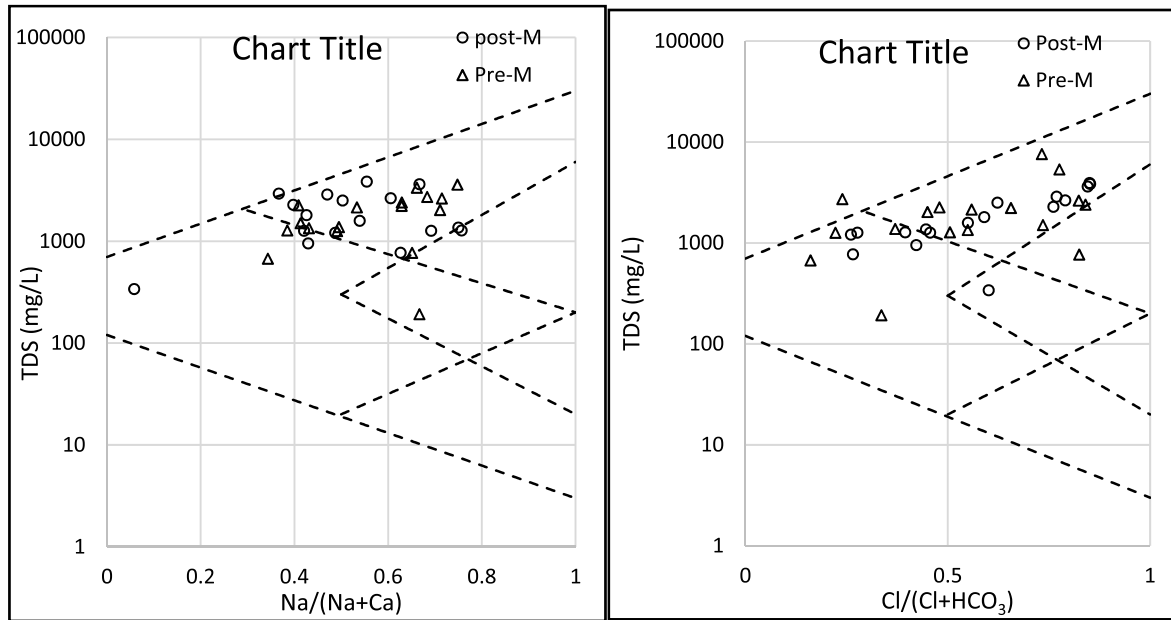


Fig. 11. Gibbs plot showing mechanisms governing groundwater chemistry.

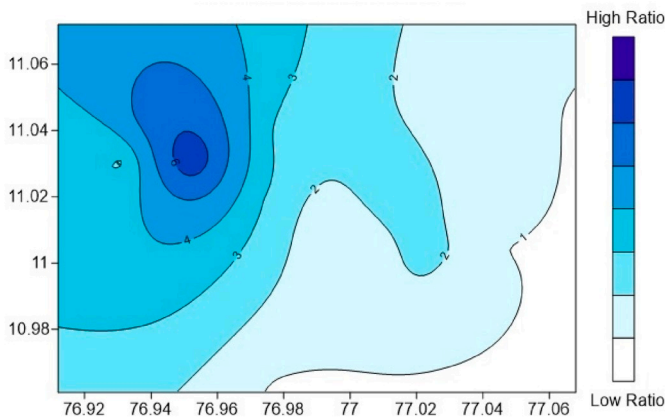
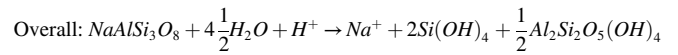
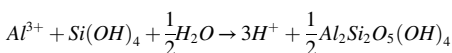
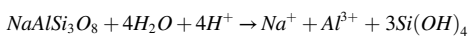


Fig. 12. Spatial distribution of Ca²⁺/Mg²⁺ ratio.

weathering (Sarin et al., 1989). Majority of the samples fall above 1:2 line while a few samples fall close to or below 1:2 line (Fig. 13(b)), thereby indicating the importance of silicate weathering only at those regions.

A constant increase in salinity with Na⁺/Cl⁻ ratio is an indicator that evaporation is a dominant process. There was a positive correlation between Ca²⁺ + Mg²⁺ and Cl⁻ (Fig. 13(c)) and a negative correlation between Na⁺/Cl⁻ and EC (Fig. 13(d)). This indicates that evaporation has no role in the hydrochemistry. Different values of Na⁺/Cl⁻ for an increasing EC suggest that exchange reactions and silicate weathering dominate over evaporation. Majority of the samples exhibited a decreasing Na⁺/Cl⁻ ratio with increasing salinity, which may be attributed to removal of Na⁺ from groundwater due to ion exchange process (Rajmohan and Elango, 2004). Further, Na⁺/Cl⁻ ratio equal to or greater than 1 suggests silicate weathering, wherein feldspar minerals under acidic conditions hydrolyze as follows:

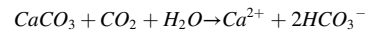


The influence of ion exchange process on the groundwater chemistry can be assessed from two chloro-alkaline indices namely CAI 1 and CAI 2 suggested by Schoeller (1967). The indices were obtained using the following equations:

$$CAI\ 1 = \frac{Cl - (Na + K)}{Cl}$$

$$CAI\ 2 = \frac{Cl - (Na + K)}{SO_4 + HCO_3 + CO_3}$$

If both the indices are positive, there is exchange of Na⁺ or K⁺ from water with Ca²⁺ or Mg²⁺ from rocks and vice versa (Schoeller, 1967). Majority of the samples exhibited a positive value of CAI 1 & CAI 2 (Fig. 13(e)), indicating that the exchange of Na⁺ or K⁺ from water occurs with Ca²⁺ and Mg²⁺ from rocks. This is in agreement with the results obtained from Ca²⁺ + Mg²⁺ vs HCO₃⁻ + SO₄²⁻ plot. For the remaining samples with negative CAI values, it is suspected that reverse ion exchange or weathering dominate over ion exchange process. During reverse ion exchange, when the replacement of Ca²⁺ & Mg²⁺ ions by Na⁺ ions in solution takes place, the removal of Ca²⁺ causes a change in pH because of the change in equilibrium of the reaction:



The reaction is driven further to the right, increasing the bicarbonate level and reduces the pH. This is depicted as shown in Fig. 13(f), wherein pH increases as the Ca²⁺ concentration drops. The overall processes occurring in the aquifer of Coimbatore city can thus be depicted as shown in Fig. 14. The ion exchange process is dominant in the south-western and central regions and major driving force for the process in this region is contamination from textile mill effluent contributing to Na⁺ ions.

4.5. Geochemical modelling

The degree of equilibrium between water and minerals in the aquifer which affects their dissolution and precipitation can best be represented by saturation index (SI). It can well predict the thermodynamic control on the composition of water which has equilibrated with the minerals in

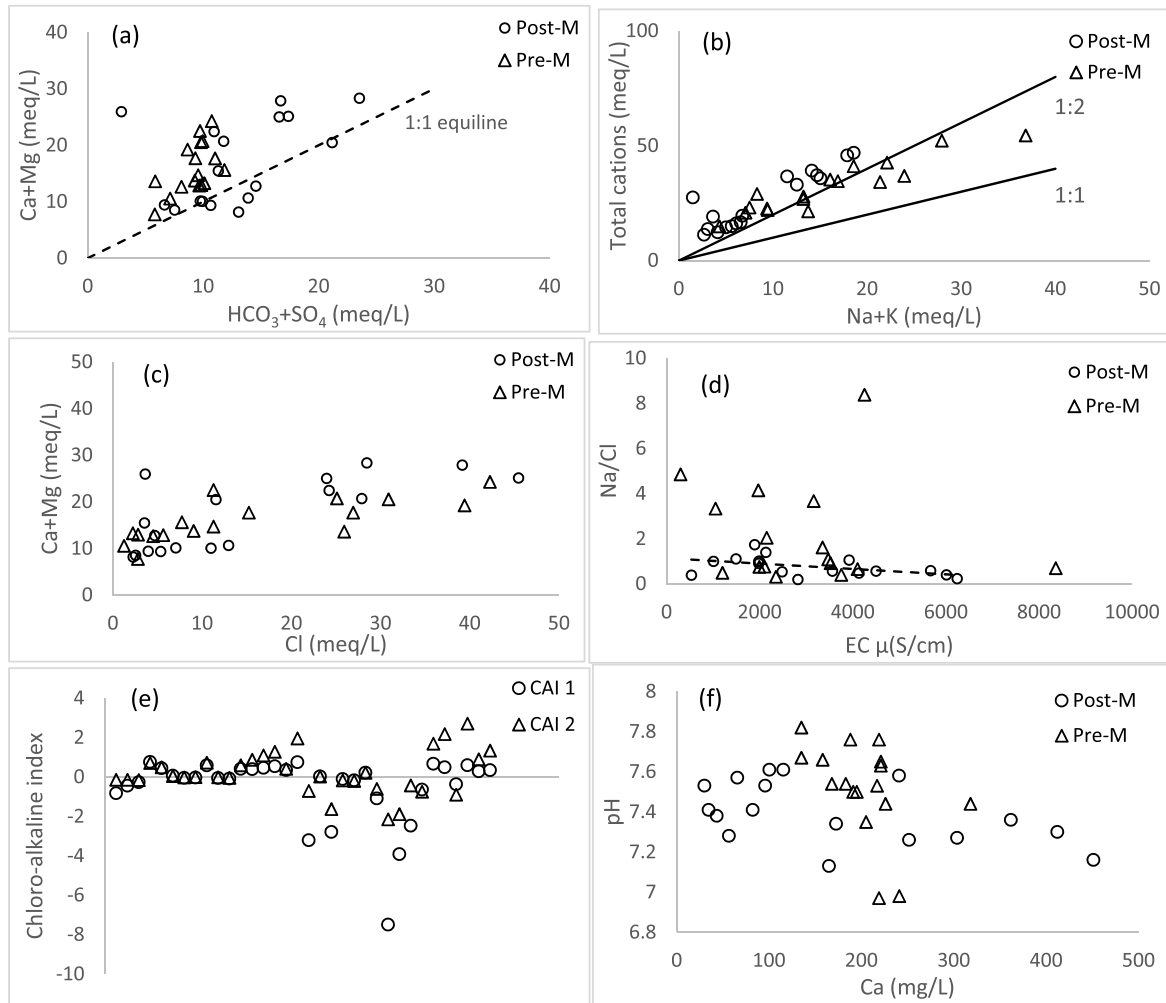


Fig. 13. Relation among major ions of groundwater from the study area.

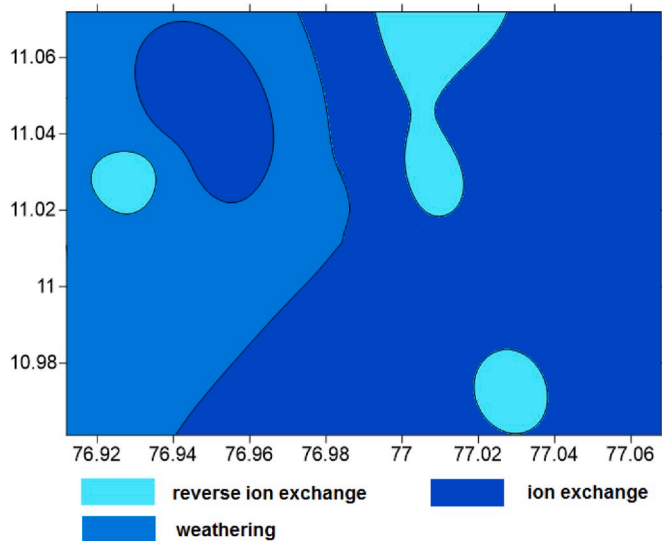


Fig. 14. Rock-water interaction occurring in the study area.

the aquifer. Saturation Index was obtained using the geochemical code PHREEQC (Parkhurst and Appelo, 1999). SI was calculated using the following expression:

$$SI = \log \left(\frac{IAP}{K} \right)$$

Where IAP is the ion activity product and K is the solubility product constant. When $SI = 0$, equilibrium exists between groundwater and minerals, while minerals tend to precipitate when they are saturated or super saturated and in such cases, SI is positive. Thus, negative SI values indicate that water is under-saturated with the minerals and suggests the possibilities of mineral dissolution. The saturation index of the groundwater samples was estimated using PHREEQC package in which the chemical parameters of the groundwater samples form the input variables. The code was run to obtain the SI of all the possible minerals. Considering the major cations and anions in the groundwater of the study area, minerals such as calcite, dolomite, aragonite were expected to dominate other minerals. The analysis of SI in the study area indicates that majority of the carbonate minerals are saturated in the aquifer (Fig. 15) and are incapable of dissolving more minerals. Of the carbonate minerals, super-saturation followed the order dolomite > calcite > aragonite. The influencing factors of super saturation of carbonate minerals include differential weathering of carbonate rocks and dissolution of silicate minerals, common ion effect (Jabal et al., 2015). This validates the previous observations that carbonate weathering dominates a major part of the study area where limestone formation is available. The other minerals including fluorite, gypsum, halite and anhydrite were under-saturated in all the samples thereby indicating that the ions such as Na^+ , Cl^- , Ca^{2+} and SO_4^{2-} were not limited by

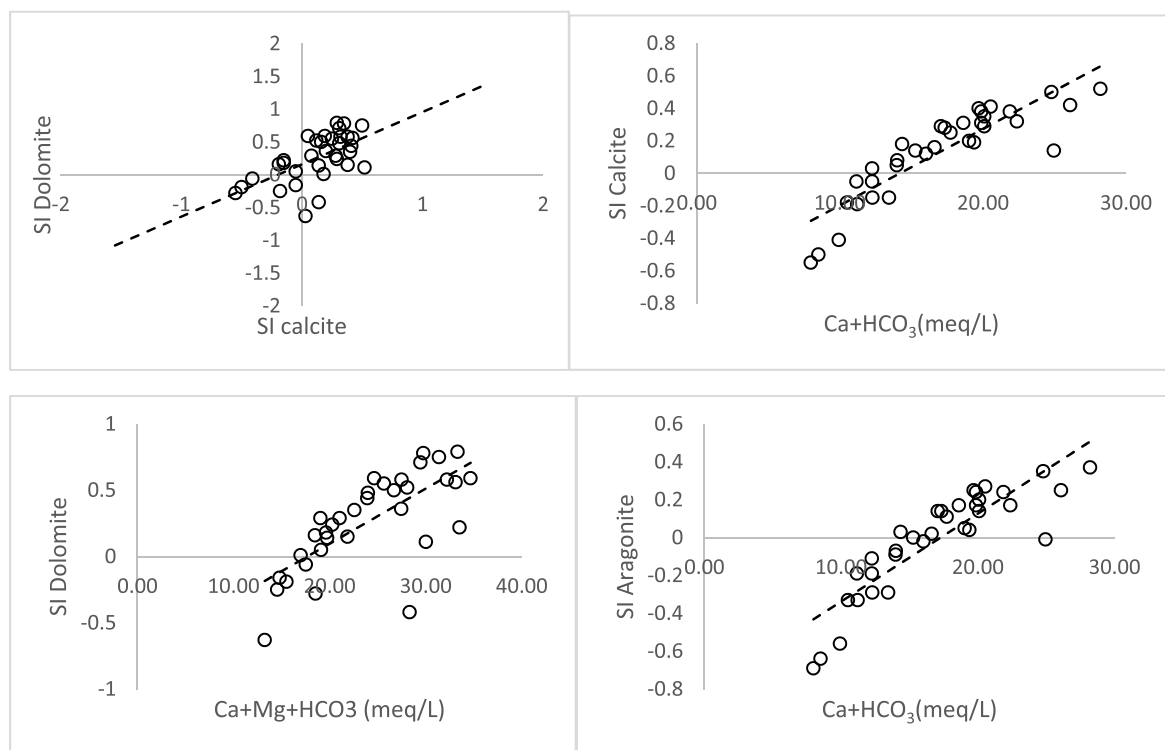


Fig. 15. Saturation indices for Calcite, Dolomite and Aragonite in the groundwater samples.

mineral equilibrium (Belkhiri and Mouni, 2013).

5. Conclusions

The study applied a multi-dimensional approach of integrating geochemical and geospatial methods to assess the processes controlling groundwater quality of Coimbatore city. The study area was dominated by Ca and Mg type of water, which get altered to Na-type or mixed Na, Ca-type over a seasonal change. The study reveals that the textile mills have played a major role in altering the water type to Na-type or mixed Na,Ca-type in the central and south-eastern regions of the city. In addition, the high concentration of Nickel on the central and south-eastern regions is contributed by the discharge of textile mill effluent into the Noyyal river, which recharge the groundwater table. The spatial distribution of Nickel and Total Dissolved Solids followed the topography of the city, thereby further validating the findings. Another major process which controls the groundwater chemistry of the region is rock-water interaction, in which ion exchange was identified to have a dominant role, followed by weathering and reverse ion exchange. The major drive for the ion exchange process is the presence of Na^+ ions, which is being supplied by the textile mills, causing an exchange for Ca ions with Na^+ ions. This is evident from the spatial distribution map showing the predominance of ion exchange process and the location of textile mills, wherein the locations where ion exchange process dominates coincide with the locations textile mills. This shows the specific application of the integration of geochemical and geospatial methods in delineating the processes in the aquifer, The results highlight that the anthropogenic activities interfere with the natural rock-water interaction in the study area. Carbonate weathering dominates silicate weathering in major parts of the study area. The assessment of saturation index for carbonate minerals such as calcite, dolomite and aragonite clearly depicts the influence of carbonate weathering. The groundwater is super saturated with these carbonate minerals, with saturation index greater than 1, while other minerals such as gypsum, halite and fluorite are unsaturated. Thus, the study revealed that the aquifer geochemical processes are influenced by the contamination from textile mills. Further

studies are demanded to quantify the transport of Nickel through the aquifer so that proper management measures can be adopted to control groundwater contamination and also for maintaining balance in the natural processes in the aquifer.

Declaration of competing interest

The authors would like to indicate that there are no conflicts of interest.

References

- Apambire, W.B., Boyle, D.R., Michel, F.A., 1997. Geochemistry, genesis, and health implications of fluoriferous groundwaters in the upper regions of Ghana. *Environ. Geol.* 33, 13–24. <https://doi.org/10.1007/s002540050221>.
- APHA, 1998. *Standard Methods for the Examination of Water and Wastewater*, 20th Editi. APHA American Public Health Association, Washington, DC.
- Baruah, M., Bhattacharyya, K.G., Patgiri, A.D., 2008. Water quality of shallow groundwater of core city area of Guwahati. In: *Proceedings of Sixteenth National Symposium on Environment*, Haryana, India, pp. 101–106.
- Belkhiri, L., Mouni, L., 2013. Geochemical modeling of groundwater in the El Eulma area, Algeria. *Desalin. Water Treat.* 51, 1468–1476. <https://doi.org/10.1080/19443994.2012.699350>.
- Demirel, Z., 2004. The history and evaluation of saltwater intrusion into a coastal aquifer in Mersin, Turkey. *J. Environ. Manag.* 70, 275–282. <https://doi.org/10.1016/j.jenvman.2003.12.007>.
- Doneen, L.D., 1964. *Water Quality for Agriculture*, vol. 48. Dep. Irrig. Univ. California, Davis.
- Elango, L., Kannan, R., 2007. Chapter 11 Rock–water interaction and its control on chemical composition of groundwater. *Dev. Environ. Sci.* 5, 229–243. [https://doi.org/10.1016/S1474-8177\(07\)05011-5](https://doi.org/10.1016/S1474-8177(07)05011-5).
- Garrels, R.M., Mackenzie, F.T., 1967. Origin of the Chemical Compositions of Some Springs and Lakes, pp. 222–242. <https://doi.org/10.1021/ba-1967-0067.ch010>.
- Gibbs, R.J., 1970. Mechanisms controlling world water chemistry. *Science* 170 (3962), 1088–1090.
- Hajjalilou, B., Khaleghi, F., 2009. Investigation of hydrogeochemical factors and groundwater quality assessment in Marand Municipality, northwest of Iran: a multivariate statistical approach. *J. Food Agric. Environ.* 7 (3&4), 930–937.
- Hem, J.D., U.S.G.S Water-Supply, 1989. In: *Study and Interpretation of the Chemical Characteristics of Natural Water*, 3rd. Paper 2254, Alexandria, Virginia, United States.
- Jabal, M.S.A., Abustan, I., Rozaimy, M.R., El Najjar, H., 2015. Groundwater beneath the urban area of Khan Younis City, southern Gaza Strip (Palestine): hydrochemistry and

- water quality. *Arab. J. Geosci.* 8, 2203–2215. <https://doi.org/10.1007/s12517-014-1346-6>.
- Jalali, M., 2007. Salinization of groundwater in arid and semi-arid zones: an example from Tajarak, western Iran. *Environ. Geol.* 52, 1133–1149. <https://doi.org/10.1007/s00254-006-0551-3>.
- Jebastina, N., Arulraj, G.P., 2016. Contamination analysis of groundwater in Coimbatore district, India: a statistical approach. *Environ. Earth Sci.* 75, 1447. <https://doi.org/10.1007/s12665-016-6253-6>.
- Jeevanandam, M., Nagarajan, R., Manikandan, M., Senthilkumar, M., Srinivasalu, S., Prasanna, M.V., 2012. Hydrogeochemistry and microbial contamination of groundwater from lower ponnaiyar basin, cuddalore district, Tamil Nadu, India. *Environ. Earth Sci.* 67, 867–887. <https://doi.org/10.1007/s12665-012-1534-1>.
- Jeong, C.H., 2001. Effect of land use and urbanization on hydrochemistry and contamination of groundwater from Taejon area, Korea. *J. Hydrol.* 253, 194–210. [https://doi.org/10.1016/S0022-1694\(01\)00481-4](https://doi.org/10.1016/S0022-1694(01)00481-4).
- Katz, B.G., Coplen, T.B., Bullen, T.D., Davis, J.H., 1997. Use of chemical and isotopic tracers to characterize the interactions between ground water and surface water in mantled karst. *Ground Water* 35, 1014–1028. <https://doi.org/10.1111/j.1745-6584.1997.tb00174.x>.
- Kaur, T., Bhardwaj, R., Arora, S., 2017. Assessment of groundwater quality for drinking and irrigation purposes using hydrochemical studies in Malwa region, southwestern part of Punjab, India. *Appl. Water Sci.* 7, 3301–3316. <https://doi.org/10.1007/s13201-016-0476-2>.
- Kelley, W.P., 1951. *Alkali Soils*. Reinhold Publishing Corporation., New York.
- Kozłowski, M., Komisarek, J., 2017. Groundwater chemistry and hydrogeochemical processes in a soil catena of the Poznań lakeland, central Poland. *J. Elem.* 22, 681–695.
- Kumar, K., Aneesh, K.K.K., 2012. Seismic microzonation of Coimbatore district using remote sensing and GIS. *Int. J. Remote Sens. GIS* 1, 99–115.
- Kumar, M., Kumari, K., Ramanathan, A., Saxena, R., 2007. A comparative evaluation of groundwater suitability for irrigation and drinking purposes in two intensively cultivated districts of Punjab, India. *Environ. Geol.* 53, 553–574. <https://doi.org/10.1007/s00254-007-0672-3>.
- Lee, J.-Y., Cheon, J.-Y., Lee, K.-K., Lee, S.-Y., Lee, M.-H., 2001. Statistical evaluation of geochemical parameter distribution in a ground water system contaminated with petroleum hydrocarbons. *J. Environ. Qual.* 30, 1548. <https://doi.org/10.2134/jeq2001.3051548x>.
- Mayo, A.L., Loucks, M.D., 1995. Solute and isotopic geochemistry and ground water flow in the central Wasatch Range, Utah. *J. Hydrol.* 172, 31–59. [https://doi.org/10.1016/0022-1694\(95\)02748-E](https://doi.org/10.1016/0022-1694(95)02748-E).
- MSME, 2013. *Brief Industrial Profile of Coimbatore District 2012-13*. Chennai, Tamil Nadu.
- Paliwal, K., 1972. *Irrigation with Saline Water*. New Delhi.
- Parkhurst, D.L., Appelo, C.A.J., 1999. *User's Guide to PHREEQC (Version 2): A Computer Program for Speciation, Batch-Reaction, One-Dimensional Transport, and Inverse Geochemical Calculations*, vol. 99. Water-Resources Investigations Report, Denver, Colorado, p. 4259. <https://doi.org/10.1234/12345678>.
- Parthasarathy, P., Someshwar Rao, M., Kumar, B., Krishan, G., Rawat, Y.S., Gupta, S., Marwah, S., Bhatia, A.K., Kaushik, Y.B., Angurala, M.P., Singh, G.P., 2012. Drinking and irrigation water quality in jalandhar and kapurthala districts, Punjab, India: using hydrochemistry. *Int. J. Earth Sci. Eng.* 5 (6), 1599–1608.
- Piper, A.M., 1944. A graphical procedure in the geochemical interpretation of water analyses, *transactions. Am. Geophys. Union* 25, 914–928.
- Priya, K.L., Arulraj, G.P., 2011. A correlation–regression model for the physicochemical parameters of the groundwater in Coimbatore city, India. *Environ. Technol.* 32, 731–738. <https://doi.org/10.1080/09593330.2010.510852>.
- Priya, K.L., Jebastina, N., Arulraj, P., 2011. Ground water quality in the Singanallur sub-basin of Coimbatore city. *J. Ind. Pollut. Contr.* 27, 15–18.
- Rajmohan, N., Elango, L., 2004. Identification and evolution of hydrogeochemical processes in the groundwater environment in an area of the Palar and Cheyyar River Basins, Southern India. *Environ. Geol.* 46, 47–61. <https://doi.org/10.1007/s00254-004-1012-5>.
- Rao, N.S., Rao, P.S., Reddy, G.V., Nagamani, M., Vidyasagar, G., Satyanarayana, N.L.V., 2012. Chemical characteristics of groundwater and assessment of groundwater quality in varaha river basin, visakhapatnam district, Andhra Pradesh, India. *Environ. Monit. Assess.* 184, 5189–5214. <https://doi.org/10.1007/s10661-011-2333-y>.
- Reddy, D.V., Nagabhushanam, P., Sukhija, B.S., Reddy, A.G.S., Smedley, P.L., 2010. Fluoride dynamics in the granitic aquifer of the Wailapally watershed, Nalgonda District, India. *Chem. Geol.* 269, 278–289. <https://doi.org/10.1016/j.CHEMGEO.2009.10.003>.
- Richards, L.A., 1954. *Diagnosis and Improvement of Saline and Alkali Soils*. U.S. Dept. of Agriculture, Washington D.C.
- Sadashivaiah, C., Ramakrishnaiah, C., Ranganna, G., Sadashivaiah, C., Ramakrishnaiah, C.R., Ranganna, G., 2008. Hydrochemical analysis and evaluation of groundwater quality in tumkur taluk, Karnataka state, India. *Int. J. Environ. Res. Publ. Health* 5, 158–164. <https://doi.org/10.3390/ijerph5030158>.
- Sajil Kumar, P.J., Elango, L., James, E.J., 2014. Assessment of hydrochemistry and groundwater quality in the coastal area of South Chennai, India. *Arab. J. Geosci.* 7, 2641–2653. <https://doi.org/10.1007/s12517-013-0940-3>.
- Saleh, A., Al-Ruwaihi, F., Shehata, M., 1999. Hydrogeochemical processes operating within the main aquifers of Kuwait. *J. Arid Environ.* 42, 195–209. <https://doi.org/10.1006/JARE.1999.0511>.
- Sarin, M., Krishnaswami, S., Dilli, K., Somayajulu, B.L., Moore, W., 1989. Major ion chemistry of the Ganga-Brahmaputra river system: weathering processes and fluxes to the Bay of Bengal. *Geochem. Cosmochim. Acta* 53, 997–1009. [https://doi.org/10.1016/0016-7037\(89\)90205-6](https://doi.org/10.1016/0016-7037(89)90205-6).
- Sawyer, G.N., McCarty, D.L., 1967. *Chemistry for Sanitary Engineers*, second ed. McGraw-Hill, New York.
- Schoeller, H., 1967. Qualitative evaluation of groundwater resources (in methods and techniques of groundwater investigation and development). *Water Resour. Ser.* 33, 44–52.
- Selvakumar, S., Chandrasekar, N., Kumar, G., 2017. Hydrogeochemical characteristics and groundwater contamination in the rapid urban development areas of Coimbatore, India. *Water Resour. For. Ind.* 17, 26–33. <https://doi.org/10.1016/J.WRI.2017.02.002>.
- Subburaj, A., 2008. *District Groundwater Brochure Coimbatore District*. Tamil Nadu, Chennai.
- Subramani, T., Rajmohan, N., Elango, L., 2010. Groundwater geochemistry and identification of hydrogeochemical processes in a hard rock region, Southern India. *Environ. Monit. Assess.* 162, 123–137. <https://doi.org/10.1007/s10661-009-0781-4>.
- Sundar, L.M., Venkatraman, S.V., Mohan, K.L., 2015. Analysis of groundwater quality around Coimbatore big tank, Tamil Nadu, India. *Int. J. Earth Sci. Eng.* 8 (2), 99–105.
- Todd, D.K., 1980. *Groundwater Hydrology*, 2nd. John Wiley and Sons, New York, p. 535.
- WHO, 2017. *Guidelines for Drinking-water Quality*, Geneva.
- Wilcox, L.V., 1955. *Classification and Use of Irrigation Waters 1–19*. USDA Circular No. 969.